

Thermoelectric power of Na-doped $\text{La}_{0.7}\text{Ca}_{0.3-y}\text{Na}_y\text{MnO}_3$ both in the presence and the absence of magnetic field

Sayani Bhattacharya, Aritra Banerjee, S. Pal, R. K. Mukherjee, and B. K. Chaudhuri

Citation: *Journal of Applied Physics* **93**, 356 (2003); doi: 10.1063/1.1527220

View online: <http://dx.doi.org/10.1063/1.1527220>

View Table of Contents: <http://scitation.aip.org/content/aip/journal/jap/93/1?ver=pdfcov>

Published by the [AIP Publishing](#)

Articles you may be interested in

Influences of the first-to-second order magnetic phase transformation on the transport properties of $\text{La}_{0.7}\text{Ca}_{0.3-x}\text{Ba}_x\text{MnO}_3$ compounds

J. Appl. Phys. **115**, 17C706 (2014); 10.1063/1.4860943

Thermoelectric properties of $\text{YBa}_2\text{Cu}_3\text{O}_{7-\delta}\text{-La}_{2/3}\text{Ca}_{1/3}\text{MnO}_3$ superlattices

Appl. Phys. Lett. **101**, 131603 (2012); 10.1063/1.4754707

Magnetic and calorimetric studies of magnetocaloric effect in $\text{La}_{0.7-x}\text{Pr}_x\text{Ca}_{0.3}\text{MnO}_3$

J. Appl. Phys. **111**, 07D726 (2012); 10.1063/1.3679441

High-temperature thermoelectric properties of $\text{Ca}_{0.9-x}\text{Sr}_x\text{Yb}_{0.1}\text{MnO}_{3-\delta}$ ($0 \leq x \leq 0.2$)

J. Appl. Phys. **105**, 093717 (2009); 10.1063/1.3125450

Improvement of the thermoelectric characteristics of Fe-doped misfit-layered $\text{Ca}_3\text{Co}_{4-x}\text{Fe}_x\text{O}_{9+\delta}$ ($x = 0, 0.05, 0.1, \text{ and } 0.2$)

Appl. Phys. Lett. **89**, 204102 (2006); 10.1063/1.2390666



Thermoelectric power of Na-doped $\text{La}_{0.7}\text{Ca}_{0.3-y}\text{Na}_y\text{MnO}_3$ both in the presence and the absence of magnetic field

Sayani Bhattacharya, Aritra Banerjee, S. Pal, R. K. Mukherjee, and B. K. Chaudhuri^{a)}

Department of Solid State Physics, Indian Association for the Cultivation of Science, Jadavpur, Kolkata-700032, India

(Received 22 April 2002; accepted 15 October 2002)

Magnetic-field ($B=0-1.5$ T) dependent thermoelectric power (TEP) of the Na-doped $\text{La}_{0.7}\text{Ca}_{0.3-y}\text{Na}_y\text{MnO}_3$ ($0.0 \leq y \leq 0.3$) system has been studied in the temperature range 80–300 K. X-ray diffraction studies indicate a rhombohedrally distorted perovskite structure of the samples. The observed sharp peak in the resistivity (ρ) versus temperature (T) curve falls and shifts to higher temperature with increasing Na concentration (y). In the low-temperature ferromagnetic (FM) regime, thermopower (Seebeck coefficient, S) obeys the expression $S = S_0 + S_{1.5}T^{1.5} + S_4T^4$ over the entire range of y . Electron-magnon scattering is found to dominate the low-temperature resistivity and TEP data. High-temperature TEP data can be well fitted with Mott's small polaron hopping model. The activation energy (E_S) and polaron hopping energy (W_H) decrease with increasing Na content. Both E_S and W_H decrease while polaron radius (r_p) increase with the application of a magnetic field. Field-dependent TEP data also indicate the suppression of spin fluctuations in the presence of a magnetic field. In the low-temperature FM region, both magnon drag and phonon drag effects coexist. © 2003 American Institute of Physics. [DOI: 10.1063/1.1527220]

I. INTRODUCTION

The recent observation of giant magnetoresistance (GMR) in films and single crystals as well as in polycrystalline samples of hole doped LaMnO_3 with the general composition $\text{R}_{1-x}\text{A}_x\text{MnO}_3$ ($R = \text{La, Pr, Nd, etc.}$ and $A = \text{Ca, Pb, Sr, Ba, etc.}$) has generated enthusiastic research efforts worldwide.¹⁻⁵ In these oxide systems, the transition from insulating to metallic states can be brought about for a wide range of doping concentrations x ($0.2 < x < 0.5$) and magnetoresistance shows a maximum around the metal-insulator transition (MIT) temperature (T_p). Above T_p , the materials show a paramagnetic insulating (PMI) phase whereas below T_p it is transformed into a ferromagnetic metallic (FMM) phase. Conventionally, the magnetic and transport properties of these materials were explained by the “double-exchange” (DE) mechanism which is controlled by the motion of the e_g electrons from Mn^{3+} to Mn^{4+} sites.⁶⁻⁸ However, Millis *et al.*⁹⁻¹¹ argued that double exchange (DE) alone could not explain the colossal magnetoresistance (CMR) and other properties like the heat-capacity anomaly around MIT and it was proposed that a strong electron-phonon (e-ph) coupling, via Jahn-Teller effects should also play an important role. Among the various transport properties of these class of materials showing MIT, thermoelectric power (TEP) is very sensitive to the nature of charge carriers, charge-carrier-spin interactions, and the thermal conductivity. The Na-doped manganites of present investigation show a very complicated behavior of the Seebeck coefficient (S) indicating both positive and negative signs depending on the temperature as well as the degree of substitution, which in turn determine the charge-carrier density of the system. In the low-temperature

FM phase, TEP is related to the changes in the electronic structures and scattering processes. In the insulating (semi-conducting) phase ($T > T_p$), the temperature-dependent TEP data provide interesting information on the energy dependence of the parameters governing the high-temperature charge transport through small polaron hopping (SPH) mechanism.¹²

Until recent times, studies of the rare-earth manganites were mostly focused on the divalent ion-doped $\text{R}_{1-x}\text{A}_x\text{MnO}_3$ compounds. Most of these compounds crystallize in an orthorhombically distorted perovskite structure (O' -type; $c/\sqrt{2} < a < b$; space-group Pbmn) with a cooperative ordering of the Jahn-Teller distorted Mn^{3+}O_6 octahedra.¹³ In contrast, there are only a few reports of transport measurements on monovalent alkali-metal ion-doped compounds like La-Na-Mn-O , La-K-Mn-O , and La-Sr-Na-Mn-O .¹⁴⁻¹⁷ To the best of our knowledge, TEP (Seebeck coefficient, S) of the Na-doped materials have not been reported so far. Alkaline-earth metal and alkali doping on LaMnO_3 can lead to different consequences, e.g., the latter can lead to less inhomogeneity, because fewer impurity ions are needed to achieve a specific carrier concentration and larger random-potential fluctuations being experienced by the electrons in the σ^* band due to the larger difference in the valence between La^{3+} and alkali-metal ions.¹⁶ Since the valence state of the alkali-metal ions is +1, substitutions with these ions result in an increase of the mixed valence of Mn^{3+} ($t_{2g}^3e_g^1; S=2$) and Mn^{4+} ($t_{2g}^3e_g^0; S=3/2$) ions which favors the DE mechanism.

In the present article, the effect of Na substitution on the thermoelectric power of $\text{La}_{0.7}\text{Ca}_{0.3-y}\text{Na}_y\text{MnO}_3$ ($0.0 \leq y \leq 0.3$) showing a y -dependent metal-insulator transition has been reported. The Seebeck coefficient (S) of different Na-doped samples ($0.0 \leq y \leq 0.3$) has been measured both in the

^{a)} Author to whom correspondence should be addressed; electronic mail: sspbkc@mahendra.iacs.res.in

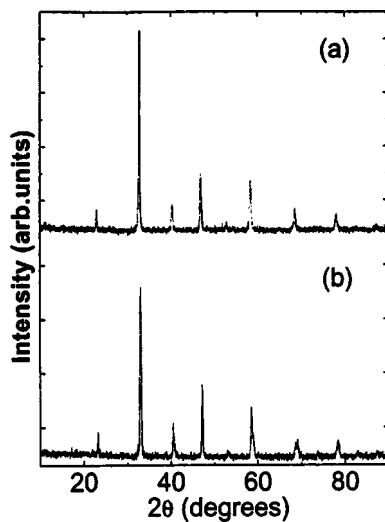


FIG. 1. XRD pattern of the two samples with (a) $y=0.0$ and (b) $y=0.15$ showing single-phase perovskite structure.

presence and absence of a magnetic field. The data are fitted to the theoretical models for a critical analysis of the salient features (carrier hopping, spin fluctuation, magnon-drag, and phonon-drag, etc.) associated with the Seebeck coefficient. For the sake of discussion, resistivities of all the samples showing MIT have also been measured.

II. EXPERIMENT

Ceramic $\text{La}_{0.7}\text{Ca}_{0.3-y}\text{Na}_y\text{MnO}_3$ ($0.0 \leq y \leq 0.3$) samples of uniform grain size were synthesized using the solid-state reaction method. Well-mixed stoichiometric amount of La_2O_3 , CaO , Na_2CO_3 , and $(\text{CH}_3\text{COO})_2\text{Mn} \cdot 4\text{H}_2\text{O}$ (each of purity $<99.9\%$) were first heated to 773 K for 5 h and then to 1073 K for another 5 h with intermediate grinding and then final heat treatment was made at 1173 K for 48 h (twice). The powder thus obtained was ground, palletized, and annealed at 1073 K for 72 h and then furnace cooled.¹⁸ The phase purity of the samples were checked by the powder x-ray diffraction (XRD) with $\text{CuK}\alpha$ radiation at room temperature. Resistivity (ρ) was measured in the 15–350 K temperature range and the thermoelectric power (S) was measured by the standard differential technique in the 80–300 K temperature range. A K -type thermocouple (corrected) was used to measure ΔT with an accuracy of ± 0.1 K.

III. RESULTS AND DISCUSSION

XRD patterns (Fig. 1) of the two typical samples with $y=0.0$ and 0.15 clearly show that all the samples are in single phase with no measurable impurity phases. The refined values of the structural parameters are given in Table I. It was observed that the undoped $\text{La}_{0.7}\text{Ca}_{0.3}\text{MnO}_3$ sample shows an orthorhombic perovskite structure with space-group Pbmn whereas, all the Na doped samples show a rhombohedrally distorted perovskite structures with $R\bar{3}c$ space group in the hexagonal axes. This is consistent with the previously reported results.^{16,17} The transition from the orthorhombic to the rhombohedral phase takes place for the sample with $y=0.05$. This particular sample ($y=0.05$) can

TABLE I. Crystallographic data of $\text{La}_{0.7}\text{Ca}_{0.3-y}\text{Na}_y\text{MnO}_3$.

y	a (Å)	b (Å)	c (Å)	α (degrees)	Space group	Structure
0.0	5.47	7.736	5.497	...	Pbmn	Orthorhombic
0.05	5.47	60.00	$R\bar{3}c$	Rhombohedral
0.10	5.46	60.31	$R\bar{3}c$	Rhombohedral
0.15	5.45	60.37	$R\bar{3}c$	Rhombohedral
0.30	5.45	60.40	$R\bar{3}c$	Rhombohedral

be indexed by both the structures. For the samples with $y > 0.05$, the structure is found to be rhombohedral. This is an interesting feature of the sample under investigation.

Figure 2 shows the resistivity (ρ) versus temperature curves of all the samples (with $y=0.0, 0.05, 0.10, 0.15$, and 0.30) showing MIT at around room temperature (except the one with $y=0.0$). In the high-temperature region (above T_p), all the samples are paramagnetic insulators (semiconductors). It is seen from Fig. 2 that with increasing y , resistivity (ρ) drops and T_p shifts to the higher-temperature region clearly indicating the extension of the FMM state because of monovalent-alkali doping in the A -site of the rare-earth manganites. This behavior of ρ can be explained by considering that with the increase of monovalent alkali doping in the A site, the number of Mn^{4+} ions among the regular Mn ions increase and hence effectively hole is injected in the conduction band. An increase in the ratio of $\text{Mn}^{4+}/\text{Mn}^{3+}$ (Table II) increases the ferromagnetic (FM) DE interaction and so the extension of the metallic state is favored. It is interesting to mention that for the samples in the lower Na doping range, a sharp MIT is observed, whereas, for the corresponding samples in the higher-doping regime, MIT peaks are relatively broader. This observation can be explained by the fact that more Na doping drives the system towards higher conductivity and the system is metallic almost throughout the temperature range. Hence, the transition from the high-temperature semiconducting phase to the low-temperature FMM phase is smoother and the resistivity peak shows a broad nature. Also, the presence of a little impure phase or different grain sizes might cause broadness of the MIT peak.

It has also been observed from the low-temperature ($T < T_p$) resistivity data of all the samples that a T^2 -dependent scattering process dominates the conduction phenomenon.¹⁸

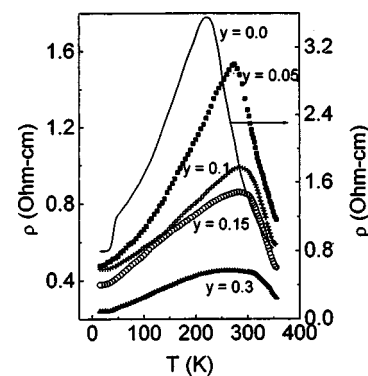


FIG. 2. Thermal variation of resistivity (ρ) of $\text{La}_{0.7}\text{Ca}_{0.3-y}\text{Na}_y\text{MnO}_3$ with $y=0, 0.05, 0.1, 0.15$, and 0.3 .

TABLE II. The values of the activation energies (E_p, E_S), hopping energy (W_H), $\text{Mn}^{4+}/\text{Mn}^{3+}$ ratio, and the constant term α' of $\text{La}_{0.7}\text{Ca}_{0.3-y}\text{Na}_y\text{MnO}_3$ in the presence and absence of magnetic field.

y	$\frac{\text{Mn}^{4+}}{\text{Mn}^{3+}}$	E_p (meV)		E_S (meV)		W_H (meV)		α'	
		0.0 T	1.5 T	0.0 T	1.5 T	0.0 T	1.5 T	0.0 T	1.5 T
0.0	0.428	116.331	91.949	13.159	9.377	103.172	82.572	-0.61	-0.45
0.05	0.538	104.593	83.869	12.757	11.343	91.836	72.526	-0.52	-0.39
0.10	0.666	97.311	79.217	11.787	10.925	85.524	68.292	-0.47	-0.35
0.15	0.818	91.915	77.197	11.601	9.635	80.314	67.562	-0.41	-0.32
0.30	1.5	85.289	75.061	10.687	9.382	74.602	65.679	-0.34	-0.28

Snyder *et al.*¹⁹ analyzed the resistivity data for Sr- and Ca-doped LaMnO_3 using the expression $\rho = \rho_0 + \rho_2 T^2 + \rho_{4.5} T^{4.5}$. Consideration of the additional $T^{4.5}$ term better fits the experimental data over a wider temperature range for both the Sr- and Ca-doped systems. Following Urushibara *et al.*,¹ the T^2 dependence of ρ in the low-temperature FM region suggests that electron-electron scattering dominates the conduction mechanism in this region and it is shown that the additional $T^{4.5}$ term arises due to the spin-wave scattering. But according to Mott,²⁰ a $\rho \sim T^2$ term does not necessarily suggest electron-electron scattering and in a ferromagnetic material, similar to our present system, the $\rho \sim T^2$ term signifies electron-magnon scattering process. So, for these samples, the electron-spin scattering process cannot be neglected in the FM regime and we attribute the T^2 term to the electron-magnon scattering process.¹⁸

Figure 3 shows the temperature-dependent thermoelectric power of different samples with $y=0.0, 0.05, 0.1, 0.15,$ and 0.3 . The thermal variation of S for the undoped sample ($\text{La}_{0.7}\text{Ca}_{0.3}\text{MnO}_3$) agrees quite well with the results reported earlier.²¹ For this sample ($y=0.0$) there is no change in the sign of the Seebeck coefficient (S) around T_p and S remain negative throughout the temperature range of our investigation. It is further noticed that the Seebeck coefficient becomes more negative with the addition of even a very small amount of sodium ($y=0.05$) in the Ca site and with the further increase of y , S tends towards a positive value finally

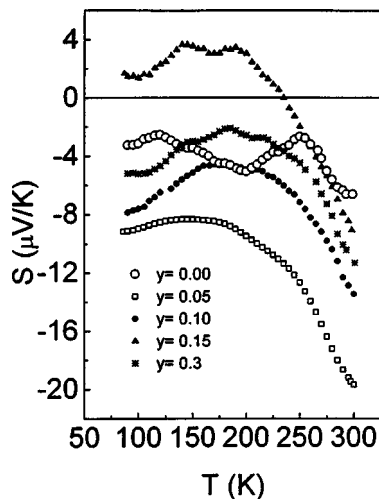


FIG. 3. Thermal variation of Seebeck coefficient (S) of $\text{La}_{0.7}\text{Ca}_{0.3-y}\text{Na}_y\text{MnO}_3$ with $y=0, 0.05, 0.1, 0.15,$ and 0.3 without applying magnetic field.

becoming positive for $y=0.15$ at low temperatures. With a further increase in the sodium content ($y=0.3$), S again decreases and remains negative throughout the temperature range. This change in S is considered to be associated with the corresponding change of Mn^{4+} content as well as with the change of the average A-site radii $\langle r_A \rangle$. With a little amount of Na doping ($y=0.05$), the Mn^{4+} ion concentration increases and S becomes more negative. Addition of further Na ions in the A site causes more hole doping which are localized in character and hence S increases (for $y=0.1$ and 0.15). This large value of thermopower arising from the hole localization may occur due to the narrowing of the e_g band due to the smaller value of $\langle r_A \rangle$ and may also be due to the distortion of the Fermi surface. The magnitudes of S for the samples with the highest ($y=0.3$) and lowest ($y=0.0$) y are almost the same. This is because the relative ratio of Mn^{3+} and Mn^{4+} (in $y=0$ sample $\text{Mn}^{3+}:\text{Mn}^{4+}=70:30$ and in $y=0.3$ sample $\text{Mn}^{4+}:\text{Mn}^{3+}=60:40$) is nearly same in both the cases. So the rate of exchange of e_g electron via the central oxygen atom (DE interaction, the key parameter controlling the transport phenomenon) is almost the same. Further, the ionic radii of Ca (0.99 \AA) and Na (0.97 \AA) ions are almost equal. These two are the most important factors in determining the sign and magnitude of S .

Figure 4 shows the variation of S with T in the presence ($B=1.5 \text{ T}$) and the absence of a magnetic field. For all the present samples, it is seen that with the application of a magnetic field ($B=1.5 \text{ T}$), S increases at low temperatures and the difference between the two values $\Delta S (=S_0 - S_{1.5})$ decreases near T_p . This indicates that the spin ordering under a magnetic field increases the thermopower of the manganite samples. The decrease in ΔS near T_p is associated with the magnetoresistance effect.

In recent times, extensive studies have been made on the polaronic transport in the high-temperature PMI phase ($T > T_p$) of rare-earth manganites.^{22,23} We also find that the high-temperature TEP data fits excellently with Mott's well-known equation¹² of the Seebeck coefficient based on polaron hopping, having the form

$$S = k_B / e [E_S / k_B T + \alpha'] \quad (1)$$

where E_S is the activation energy obtained from the TEP data and α' is a constant of proportionality between the heat transfer and the kinetic energy of an electron, where $\alpha' < 1$ suggests hopping due to small polarons and $\alpha' > 2$ suggests the existence of large polarons.²⁴ Figure 5 give the S versus $1/T$ curve for all the samples both in the presence and ab-

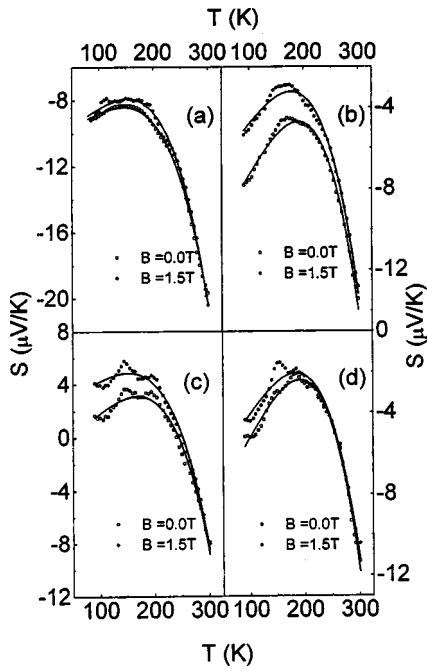


FIG. 4. Temperature and magnetic-field dependent Seebeck coefficient (S) of four different samples with (a) $y=0.05$, (b) 0.1, (c) 0.15, and (d) 0.3. Solid lines are best-fit lines to the Eq. (4).

sence of a magnetic field. Solid line gives the best fit of the experimental data with Eq. (1). From the slope of S versus $1/T$ curves, we obtain the values of the activation energy E_S for all the samples. The constant α' is obtained from the intercept of the plotted curves. All the parameters obtained from fitting the experimental data with Eq. (1) are given in Table II. From the estimated values of α' [from Eq. (1)], we find $\alpha' < 1$ for both 0.0 and 1.5 T magnetic field. This supports the small polaron hopping conduction mechanism in this system. For the sake of completion and discussion, the values of the activation energy (E_p) obtained from fitting the high-temperature resistivity data with Mott's equation¹² viz.

$$\rho/T = \rho_\alpha \exp(E_p/k_B T) \quad (2)$$

are also shown in Table II. The calculated values show that both the activation energies (E_p and E_S) gradually decrease with increasing sodium content. For a certain y , the activation energy is found to decrease in the presence of a magnetic field. The difference in the values of the two activation energies (E_p and E_S), as originally pointed out by Mott and Davis, is the thermally activated behavior of the hopping transport at high temperature. The difference between the activation energies, measured from resistivity and TEP studies, is then the polaron hopping energy $W_H = E_p - E_S$. The calculated values of the hopping energy, both in the absence ($B=0$ T) and the presence ($B=1.5$ T) of a magnetic field are shown in Table II. A decrease of all the parameters E_p , E_S , and W_H with increasing y imply that increasing Na concentration sufficiently increases the number of charge carriers and this increased number of carriers (holes) in the e_g band take part in conduction thereby reducing the energy needed to release a charge carrier. This effectively reduces

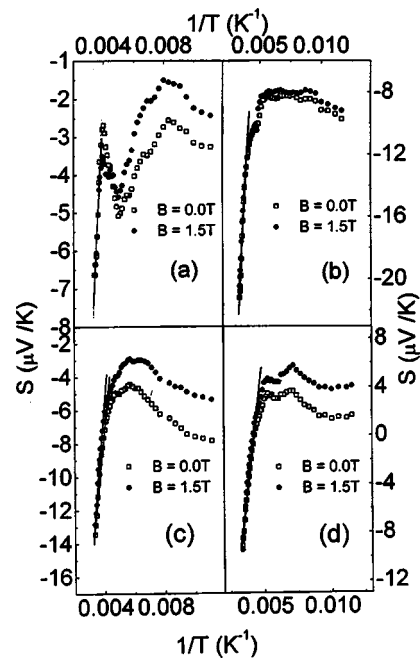


FIG. 5. S vs $1/T$ plot for four different samples with (a) $y=0.0$, (b) 0.05, (c) 0.1, and (d) 0.15. Solid lines are best-fit lines to the Mott's equation [Eq. (1)].

the activation and the hopping energy. According to Mott and Davis,¹² the hopping energy W_H is related to the polaron radius (r_p) as

$$W_H = e^2/4\epsilon(1/r_p - 1/R), \quad (3)$$

where ϵ is the dielectric constant and R is the average inter-site distance related to r_p ($r_p = (\pi/6)^{1/3}R/2$). With the application of a magnetic field, hopping energy W_H decreases and hence the polaronic radius increases (as r_p is inversely proportional to W_H). Mott and Austin²⁵ also showed that for finite disorder energy between the occupied and unoccupied sites, α' is given by $\alpha' = (W_H/kT)(1 - \theta)/(1 + \theta)$, where θ is a constant related to the amount of disorder in the system. $\theta = 1$ suggests zero disorder whereas any deviation of θ from 1 is a measure of the disorder in the system. The present series of samples show $\theta \sim 0.7-0.8$ (depending on y), quite close to the value predicted by Mott and Austin ($\theta \sim 0.9$). The application of a magnetic field increases θ thereby reducing the amount of disorder in the manganite system, which is further confirmed, by the increase of conductivity with the application of a magnetic field.

The resistivity and the TEP values of the undoped sample $\text{La}_{0.7}\text{Ca}_{0.3}\text{MnO}_3$ have already been studied and the temperature dependence of S below T_p has been expressed by the relation²⁶

$$S = S_0 + S_{1.5}T^{1.5} + S_4T^4 \quad (4)$$

where S_0 is a constant term inserted to account for the problem of truncating the low-temperature data. The low temperature (FM phase) TEP data of the samples ($y=0.0, 0.05, 0.10, 0.15$, and 0.30) are well fitted with Eq. (4) as shown in [Figs. 4(a)–4(d)]. The corresponding fitting parameters for the samples are shown in Table III for comparison. For all the samples $S_{1.5} \gg S_4$, which suggests that at low tempera-

TABLE III. The values of the parameters S_0 , $S_{1.5}$, and S_4 obtained from fitting the low-temperature (ferromagnetic phase) thermoelectric power data with Eq. (4) both in the presence and in absence of magnetic field.

y	S_0 ($\mu\text{V/K}$)		$S_{1.5}$ ($\mu\text{V/K}^{2.5}$)		S_4 ($\mu\text{V/K}^5$)	
	0.0 T	1.5 T	0.0 T	1.5 T	0.0 T	1.5 T
0.00	-3.839	-3.707	2.34×10^{-3}	2.3×10^{-3}	-4.10×10^{-9}	-5.69×10^{-9}
0.05	-11.173	-9.927	2.27×10^{-3}	1.7×10^{-3}	-2.44×10^{-9}	-2.36×10^{-9}
0.10	-10.406	-7.385	3.42×10^{-3}	2.8×10^{-3}	-2.63×10^{-9}	-2.51×10^{-9}
0.15	1.909	2.478	2.72×10^{-3}	2.13×10^{-3}	-2.98×10^{-9}	-2.97×10^{-9}
0.30	-7.228	-6.846	3.18×10^{-3}	3.05×10^{-3}	-2.57×10^{-9}	2.47×10^{-9}

tures, the temperature dependence of S is governed by the second term in Eq. (4) which arises due to electron-magnon scattering contribution. However, at high temperatures the T^4 term (spin-wave fluctuation contribution) cannot be neglected and this term actually fits the data [with Eq. (4)] over this region. It was also noticed from the resistivity data¹⁸ that the electron-magnon scattering process dominates the conduction mechanism in the low-temperature (FM phase) range. Therefore, from the TEP measurements it is confirmed that the electron-magnon scattering process is predominant in the low-temperature FM phase. At low temperatures, an almost linear dependence of S with $T^{3/2}$ is observed for all the samples. A similar result is also reported by Jaime *et al.*²⁷ for the $\text{La}_{0.67}(\text{Ca/Pb})_{0.33}\text{MnO}_3$ -type single crystal. In this region (below 80 K), they observed S linearly increases with T

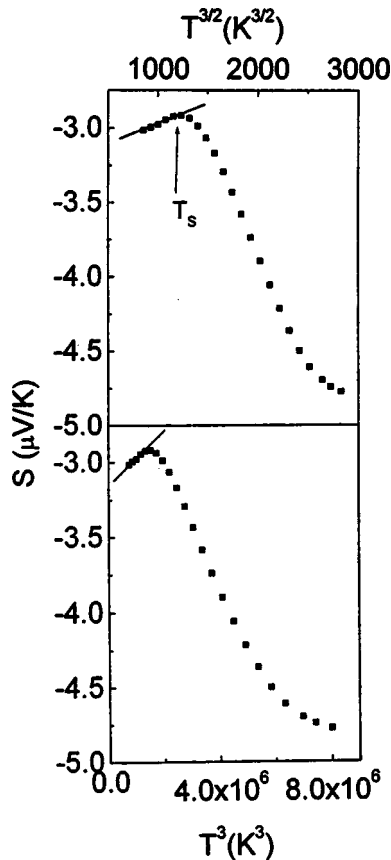


FIG. 6. S vs $T^{1.5}$ and S vs T^3 plot for the sample $\text{La}_{0.7}\text{Ca}_{0.3}\text{MnO}_3$. An almost linear variation of S with $T^{1.5}$ and T^3 below T_S suggest the presence of both phonon and magnon drag effects in the low-temperature region.

and the S versus T curve showed a positive curvature in the temperature range 30–80 K. For our samples, the temperature up to which linearity is seen in the S versus $T^{3/2}$ curve, increases with the increase in Na doping concentration, and the S value reaches a maximum at a temperature $T=T_S$ (say). Above this temperature, the curve shows a negative slope and decreases almost linearly with $T^{3/2}$ thereby exhibiting a peak at around T_S (Fig. 6). Blatt *et al.*²⁸ showed similar behavior of thermopower for metallic Fe and explained this behavior by applying the magnon drag theory, similar to the phonon drag theory. They also predicted that at low temperatures, phonon drag (S_g) and magnon drag (S_m) contributions are present and should be proportional to their respective specific heat contributions so that $S_g \propto T^3$ and $S_m \propto T^{3/2}$. A linear dependence of S with $T^{3/2}$ as well as T^3 (Fig. 6) is observed in our present samples which suggests that in the low-temperature ferromagnetic phase, a magnon drag is produced due to the presence of electron-magnon interaction along with the effect of phonon drag due to electron-phonon interaction. From the error calculation of the fitting parameters, it is seen that the effect of phonon drag on the transport properties in this temperature range (80 K- T_S) is marginally greater than the magnon drag effect. However, there is almost no effect of magnetic field on the T_S value which further indicates the predominance of phonon drag in the present system for the above-mentioned temperature range. The magnon drag effect is only predominant at much lower ($20 < T < 80$ K) temperature range. The presence of the thermopower peak near $\theta_D/5$ for all the samples (where Debye temperature θ_D varies from 510.2–657.9 K for the present system) is also a concrete proof of phonon drag effect in the present system.²⁶ However, the magnon drag effect cannot be neglected due to strong electron-magnon interaction in the system (from resistivity and TEP fitting). It is getting only gradually suppressed as the temperature is heading towards MIT. For all the samples of present investigation, S_0 [Eq. (4)] is found to increase in the presence of a magnetic field. Magnetic field decreases the coefficient $S_{3/2}$ for all the samples ($y=0, 0.05, 0.1, 0.15$, and 0.3) which strongly supports that the electron-spin scattering process is suppressed due to the external magnetic field. However, the interdependency of the parameters S_0 , $S_{3/2}$, etc. is not well known and for such information, a more detailed study of thermopower under a high-magnetic field is needed.

IV. CONCLUSION

In conclusion, magnetic-field-dependent electrical conductivity and thermoelectric power of the monovalent alkali (Na) doped $\text{La}_{0.7}\text{Ca}_{0.3-y}\text{Na}_y\text{MnO}_3$ system ($y=0-0.3$) supports small polaron hopping (SPH) conduction mechanism above the respective MIT temperature (T_p). Below T_p , the magnetic-field-dependent TEP data can be well fitted with the equation of the form $S=S_0+S_{1.5}T^{1.5}+S_4T^4$, where the second term suggests the importance of electron-magnon scattering in the low-temperature FMM phase. Electron-magnon scattering is also indicated from low-temperature resistivity data. The suppression of $S_{1.5}$ in the presence of the magnetic field suggests that electron-spin scattering decreases with the application of the magnetic field. The importance of the spin-wave fluctuation (T^4 term) is visible in the high-temperature range. The low-temperature linear dependence of S with $T^{1.5}$ and T^3 suggests the presence of both the magnon and phonon drag effects in the low-temperature FM phase. Finally, the study of field-dependent thermopower, heat capacity, and conductivity of manganite would be interesting for a deeper understanding of the magnon and phonon drag effects in such materials.

ACKNOWLEDGMENTS

The authors are grateful to the Department of Science and Technology, Government of India, for financial support. Also, a valuable discussion with Dr. Sandip Chatterjee is gratefully acknowledged.

- ¹A. Urushibara, Y. Moritomo, T. Arima, A. Asamitsu, G. Kido, and Y. Tokura, *Phys. Rev. B* **51**, 14 103 (1995).
- ²R. van Helmolt, J. Wecker, B. Holzapfel, L. Schultz, and K. Samwer, *Phys. Rev. Lett.* **71**, 2331 (1995). W. Prellier, Ph. Lecoeur, and B. Mercey, *J. Phys.: Condens. Matter* **13**, R915 (2001).
- ³M. McCormack, S. Jin, T. Tiefel, R. M. Fleming, J. M. Phillips, and R. Ramesh, *Appl. Phys. Lett.* **64**, 3045 (1994).
- ⁴R. Ramesh, R. Mahendiran, A. K. Raychaudhuri, and C. N. R. Rao, *J. Solid State Chem.* **114**, 297 (1995).

- ⁵H. L. Ju, J. Gopalakrishnan, J. L. Peng, Q. Li, G. C. Xiong, T. Venkatesan, and R. L. Greene, *Phys. Rev. B* **51**, 6143 (1995).
- ⁶C. Zener, *Phys. Rev.* **82**, 403 (1951).
- ⁷P. W. Anderson and H. Hasegawa, *Phys. Rev.* **100**, 675 (1955).
- ⁸P.-G. de Gennes, *Phys. Rev.* **118**, 141 (1960).
- ⁹A. J. Millis, P. B. Littlewood, and B. I. Shraiman, *Phys. Rev. Lett.* **74**, 5144 (1995).
- ¹⁰A. J. Millis, *Phys. Rev. B* **53**, 8434 (1996).
- ¹¹A. J. Millis, B. I. Shraiman, and R. Mueller, *Phys. Rev. Lett.* **77**, 175 (1996).
- ¹²N. F. Mott and E. A. Davis, in *Electronics Process in Non Crystalline Materials* (Clarendon, Oxford 1971).
- ¹³J. A. M. van Roosmalen, P. van Vlaanderen, and E. H. P. Cordfunke, *J. Solid State Chem.* **114**, 516 (1995).
- ¹⁴C. Boudaya, L. Laroussi, E. Dhahri, J. C. Joubert, and A. Cheikhrouhou, *J. Phys.: Condens. Matter* **10**, 7485 (1998).
- ¹⁵G. H. Rao, J. R. Sun, K. Bärner, and N. Hamad, *J. Phys.: Condens. Matter* **11**, 1523 (1999).
- ¹⁶N. Abdelmoula, A. Cheikhrouhou, and L. Reversat, *J. Phys.: Condens. Matter* **13**, 449 (2001).
- ¹⁷S. Roy, Y. Q. Guo, S. Venkatesh, and N. Ali, *J. Phys.: Condens. Matter* **13**, 9547 (2001).
- ¹⁸Sayani Bhattacharya, Aritra Banerjee, S. Pal, P. Chatterjee, R. K. Mukherjee, and B. K. Chaudhuri, *J. Phys.: Condens. Matter* (to be published).
- ¹⁹G. J. Snyder, R. Hiskes, S. DiCarolis, M. R. Beasley, and T. H. Geballe, *Phys. Rev. B* **53**, 14 434 (1996).
- ²⁰N. F. Mott, *Metal-Insulator Transitions* (Taylor and Francis, London, 1974).
- ²¹R. Mahendiran, S. K. Tiwary, A. K. Raychaudhuri, T. V. Ramakrishnan, R. Mahesh, N. Rangavittal, and C. N. R. Rao, *Phys. Rev. B* **53**, 3348 (1996).
- ²²M. Jaime, M. B. Salamon, K. Pettit, M. Rubenstein, R. E. Treece, J. S. Horwitz, and D. B. Chrisey, *Appl. Phys. Lett.* **68**, 1576 (1996); S. Chatterjee, P. H. Chou, C. F. Chang, I. P. Hong, and H. D. Yang, *Phys. Rev. B* **61**, 6106 (2000).
- ²³M. Jaime, M. B. Salamon, M. Rubenstein, R. E. Treece, J. S. Horwitz, and D. B. Chrisey, *Phys. Rev. B* **54**, 11 914 (1996).
- ²⁴Aritra Banerjee, S. Pal, S. Bhattacharya, B. K. Chaudhuri, and H. D. Yang, *Phys. Rev. B* **64**, 104 428 (2001).
- ²⁵N. F. Mott and I. G. Austin, *Adv. Phys.* **18**, 41 (1969).
- ²⁶P. Mandal, *Phys. Rev. B* **61**, 14 675 (2000).
- ²⁷M. Jaime, P. Lin, M. B. Salamon, and P. D. Han, *Phys. Rev. B* **58**, R5901 (1998).
- ²⁸F. J. Blatt, D. J. Flood, V. Rowe, and P. A. Schroeder, *Phys. Rev. Lett.* **18**, 395 (1967).